Hindawi
Advances in Civil Engineering
Volume 2022, Article ID 4298933, 12 pages
https://doi.org/10.1155/2022/4298933

Research Article

Response Surface-Based Finite Element Model Updating of Steel Box-Girder Bridges with Concrete Composite Decks

Cheng-Qi Xiong, Zhi-Wen Zhu, and Jin Jiang

Department of Civil and Environmental Engineering, Shantou University, Shantou 515063, China

Correspondence should be addressed to Zhi-Wen Zhu; zhuzw@stu.edu.cn

Received 20 October 2022; Revised 30 October 2022; Accepted 2 November 2022; Published 8 December 2022

Academic Editor: Ying Qin

Copyright © 2022 Cheng-Qi Xiong et al. This is an open access article distributed under the Creative Commons Attribution License, which permits unrestricted use, distribution, and reproduction in any medium, provided the original work is properly cited.

The orthotropic steel deck (OSD) using the steel-steel fiber reinforced concrete (SFRC) deck can be used in small and medium-span bridges for its advantages of construction convenience and lower construction cost. The seismic performance of THESE steel box girder bridges in strong earthquake zones needs to be evaluated, and a reasonable finite element model is the important basis for an accurate evaluation of these bridges. Finite element analysis (FEA) and field measurements of the dynamic characteristics of steel box girder bridges were carried out in this study, and the finite element model was updated based on the response surface method. The studies show that the bridge modal parameters can be reasonably identified based on the measurements of the bridge under ambient excitation without artificial excitation; the first six orders of mode shapes in the FEA results are consistent with the measured ones, but there is a difference between the natural frequencies; the model updating found that the elasticity modulus, density, and thickness of the SFRC have some influence on the first six orders of natural frequency of the bridge, but the SFRC thickness has the most significant influence on the bridge frequency, and the influence of epoxy asphalt pavement on bridge frequency is small. The study concluded that the SFRC layer of the bridge deck is no longer the traditional bridge deck pavement without considering the stiffness, but it integrates with the OSD as a steel-concrete composite structure. Therefore, the structure formed by the SFRC layer through the combination of shear studs and OSD shall be reasonably simulated in the finite element model so as to reasonably reflect the contribution of the SFRC layer in the composite structure of the bridge stiffness. The obtained updated finite element model gives results closer to the measured modalities, which provides a more reasonable bridge model for seismic analysis of bridges located in strong seismic zones and also demonstrates the effectiveness of the finite element analysis and the model updating method based on the response surface method in this study.

1. Introduction

Orthotropic steel bridge decks (OSDs) consist of welded deck plate, longitudinal ribs, and diaphragms and have been widely used in bridge engineering worldwide [1]. This structure features a large number of weld joints, complex structure and stress, low local stiffness, and significant stress concentration. Under the action of concentrated wheel load, the local stress range at connection details is high, and fatigue cracks may initiate and propagate at connection details [2–5]. One of the important reasons is that the traditional OSDs adopt epoxy pavement. When the temperature is low, the elastic modulus of this pavement material is high, which together with the large thickness provides greater additional stiffness for the OSDs, thereby reducing the stress range of the fatigue-prone details of the OSDs. However, when the ambient temperature is high and the solar radiation is strong, the temperature of the pavement layer may be very high, and its elastic modulus will decrease significantly [6]; therefore, it cannot contribute additional stiffness to the OSDs. Under such situation and concentrated wheel load, the fatigue-prone details of OSDs will produce a high stress range, leading to the initiation and propagation of fatigue cracks. At the same time, the high temperature can also cause the softened epoxy pavement to shift and debond with the OSDs, leading to pavement damage. Fatigue and cracking of

OSD details affect the safety and durability of bridges, while frequent pavement layer replacement will present serious impact on local transportation.

Concrete materials have the advantages of large elastic modulus and high compressive strength, as well as disadvantages of low tensile strength and easy cracking. Steel fiber reinforcement concrete (SFRC) is a kind of multiphase composite material formed by mixing short steel fibers randomly in ordinary concrete. Within SFRC, the randomly distributed steel fibers can prevent the expansion of microcracks and the formation of macrocracks in concrete and improve the tensile strength of concrete by 40% ~ 80%. With the reinforced SFRC layer adopted to form a steel-SFRC composite structure with the OSDs by means of intralayer shear studs, the stress at the OSD connection details is significantly reduced, and the risks of cracking and debonding the bridge deck pavement get lowered [7].

Based on finite element analysis of bridge dynamics [8], one can not only obtain a reasonable finite element model but also can accurately obtain modal damping ratio of the bridge. As the finite element analysis can only obtain the frequencies and mode shapes that reflect the stiffness and mass distribution characteristics of the bridge and its rationality needs to be verified by actual bridge data, when the results are inconsistent with the measured results, the model needs to be updated by a reasonable method. The SFRC layer in OSDs with steel-SFRC composite structures should be able to improve the local stiffness of the bridge decks to a certain extent, but its reasonable reflection in the finite element model and the damping characteristics of this new bridge deck structure have not yet been reported in studies. Therefore, updating on the finite element model of bridges is of great significance to subsequent analysis of bridge dynamics.

In recent years, the response surface method (RSM) and its improved methods have been applied in the field of model updating [8–13]. In this paper, based on an actual OSD steel box girder bridge with steel-SFRC composite structures, we used the reference-based cross-point power spectrum method, picked up the bridge vibration signals under ambient excitation, and used the cross-point power spectrum method to identify the modal parameters of the dynamic response signals of the structure [14], and thereby obtained the modal frequencies, damping ratio, and mode shapes of the bridge. Then we compared the findings with the ANSYS model and updated the model by the response surface method, thus providing a reasonable finite element model for the seismic analysis of the bridge in the strong earthquake area.

2. Principle of Response Surface-Based Model Updating

The response surface method combines statistics with mathematics. Through several numerical experiments, the implicit relationship between structural parameters and structural response is established by the explicit function, and then the response surface model is established based on this function. The structural response is obtained by inputting structural parameters to the response surface model, and the finite element analysis is no longer carried out so as to obtain reasonable structural response. This method includes experimental design, parameter screening, significance analysis, response surface model fitting, and parameter optimization [13].

In order to determine the reasonable structural parameters and improve the efficiency of model updating, we carried out ANOVA [15, 16] by the F-test method and selected parameters that were significant to the model, which overcome the shortcomings of the traditional sensitivity analysis method that only calculates local sensitivity [9]. The formula is as shown below:

$$F = \frac{\mathrm{SSA}/J_m}{\mathrm{SSE}/J_n} \sim F(J_m, J_n), \tag{1}$$

where SSA is the sum of squares of bridge frequency deviations caused by different levels of parameters (including system errors and random errors), SSE is the sum of squares of bridge frequency deviations caused by test errors under the same level of parameters (only including random errors), J_m is $r-1$ (r is the number of levels of parameters), and J_n is $n-r$ (n is the total number of tests); the value of the significance evaluation parameter P corresponding to statistic F is calculated, taking the significance level $\alpha = 0.05$. If the P value is greater than α, the change of the parameter has no significant effect on the result; otherwise, the parameter should be updated.

In this study, we used the Box–Behnken design (BBD) method to construct parameter samples to be updated and used the ANSYS finite element software to obtain characteristic quantity samples under different parameter values. Taking the SFRC elastic modulus, density, thickness, elastic modulus of steel of the steel box girders, and the epoxy asphalt temperature of the OSDs of a bridge as the input values and the frequency of each order of the bridge mode as the output values, a response surface model was constructed to fit the implicit function relationship between the characteristic values and the selected parameters.

We employed the second-order polynomial response surface model as follows:

$$y_{RS} = \beta_0 + \sum_{i=1}^{k} \beta_i x_i + \sum_{i=1}^{k} \sum_{j=1}^{k} \beta_{ij} x_i x_j + \sum_{i=1}^{k} \beta_{ii} x_i^2, \tag{2}$$

where, in $x_i \in [xl/i, xu/i]$, xl/i and xu/i are the upper and lower limits of the design parameter x_i, $\beta_0, \beta_i, \beta_{ij}$, and β_{ii} are the regression coefficients, k is the number of parameters screened out by the ANOVA, and y_{RS} is the calculation result of the second-order polynomial response surface model.

After obtaining the response surface model, it was necessary to verify the rationality of the model, and two indicators were used, namely,

$$R^2 = 1 - \frac{\sum_{j=1}^{N} [y_{RS}(j) - y(j)]^2}{\sum_{j=1}^{N} [y(j) - \overline{y}]^2},$$
$$\text{RMSE} = \frac{1}{\sqrt{y}} \sum_{j=1}^{N} [y_{RS}(j) - y(j)]^2, \quad (3)$$

wherein y_{RS} and y represent the results of the response surface model calculation and the finite element analysis, respectively, N is the number of check points, and $\overline{y}$ is the average value of the finite element analysis results. The root mean square error (RMSE) is closer to 0, or the multiple correlation coefficient R^2 is closer to 1, then the accuracy of the response surface model is higher.

The finite element model updating can be regarded as optimization [13] in essence, of which the key elements are the construction of the target function and the selection of the optimization algorithm. Considering that the higher the order, the greater the corresponding frequency in the bridge modal analysis in order to ensure the updating effect at each order, and the target function as shown in formula (4) was established:

$$f = \min \sum_{i=1}^{m} \left| 1 - \frac{y_{RS}(x_i)}{f_{Ei}} \right|, \quad (4)$$

$$s.t. x_i^l \ll x_i \ll x_i^u, \quad (5)$$

where f_{Ei} is the measured value of order i and $y_{RS}(x_i)$ is the response surface analysis value at order i.

The appropriate optimization algorithm is the premise of reasonable updating of the model. The genetic algorithm (GA) can overcome dead cycles in iterative operation [17, 18] and is a global optimization algorithm. Therefore, it was selected as the optimization algorithm, and the measured frequency values were taken as the updating targets. Within the reasonable range of parameters, the quadratic polynomial response surface model was subjected to optimized iterative calculation, and finally, the parameter optimization values were obtained.

3. Overview of the Bridge

The Leiguang Overpass Bridge is located at the intersection of G324 Highway and Leiguang Road in Shantou City. It is a multispan steel box girder bridge. The bridge span consists of $2 \times 30 + 35 + 60 + 35 + 2 \times 30$ m, and the elevation layout is as shown in Figure 1. The tested section is the south approach bridge, with two equal spans of 30 m. The main girder is a single box, double chambers steel box girder. The main girder at the center line of the road is 1.6 m high, and the bridge deck is 19 m in design width, with two-way four lanes. The bridge top consists of OSDs and is set with 2.0% bidirectional transverse slopes. The main girder bottom plate is horizontal. A 13 cm thick reinforced SFRC layer is laid on the OSDs and fixed to the OSDs by shear studs to form an OSD structure with a steel-SFRC composite deck, and 9 cm thick epoxy asphalt concrete is paved on the top. Central and roadside anticollision steel barriers are set on the deck, the steel of the main girder is Q345qD, and the lower structure is a double-column pier with the cover beam. As the bridge is located in Shantou, a strong earthquake area, it needs to be evaluated for antiseismic performance. Hence, a reasonable finite element model is important to carry out such kind of investigation.

4. Dynamic Characteristics Analysis of the Initial Finite Element Model

According to the design drawings, an initial finite element model of the south approach bridge as shown in Figure 1 was established. The origin of the coordinate system is located at the end of the abutment beam in the middle line of the bridge, the x-axis is along the bridge direction, the y-axis is vertical, and the z-axis is in bridge transverse direction. The fishbone finite element modeling strategy was adopted to separate the mass and stiffness of the main girder, in which the element type Beam4 was used as the ridge beam to simulate the stiffness of the main girder, and the element type Mass 21 was used to simulate the translating and rotating mass of the main girder. The initial material parameters are as follows: the elastic modulus of steel was 2.1×10^5 MPa, the density was 7850 kg/m^3, and Poisson's ratio was 0.3, the elastic modulus of C40 steel fiber reinforced concrete was 3.45×10^4 MPa, the density was 2400 kg/m^3, Poisson's ratio was 0.167, and the elastic modulus of epoxy pavement was determined at the temperature of 30°C. The main girder was divided into 41 segments longitudinally. In order to show the torsion mode shape of the main girder, fishbone elements were arranged on both sides of the fishbone, and rigid arm elements without weight were used for simulation. All the translational degrees of freedom and the rotational degrees of freedom around the X and Y-axes of elements 1 and 41 were constrained, respectively, and all the translational degrees of freedom and the rotational degrees of freedom around the Y axis of element 21 were constrained to simulate the actual constraints. The initial finite element model is shown in Figure 2. The first six natural frequencies and mode shapes obtained by dynamic characteristic analysis are shown in Table 1.

Figure 3 shows the first six order mode shapes obtained by finite element analysis. It can be seen that the bridge has a fundamental frequency of 3.77 Hz at the first-order asymmetric bending mode in the vertical direction, indicating that the main girder has the smallest stiffness in the vertical direction, which may be related to the lower height of the main girder; it has a second-order frequency of 4.99 Hz at the first-order symmetrical bending mode in the vertical direction; and it has a third-order frequency of 5.3 Hz at the first-order symmetric torsional mode. The subsequent third-order mode shapes are all torsional modes of the main girder, and the first six order modes show no lateral mode of the bridge, which may be related to the large lateral stiffness caused by the large width of the main girder. The third to sixth order are torsional vibration modes, indicating that the torsional stiffness of the bridge is small, which may be related to the lower height of the main girder.

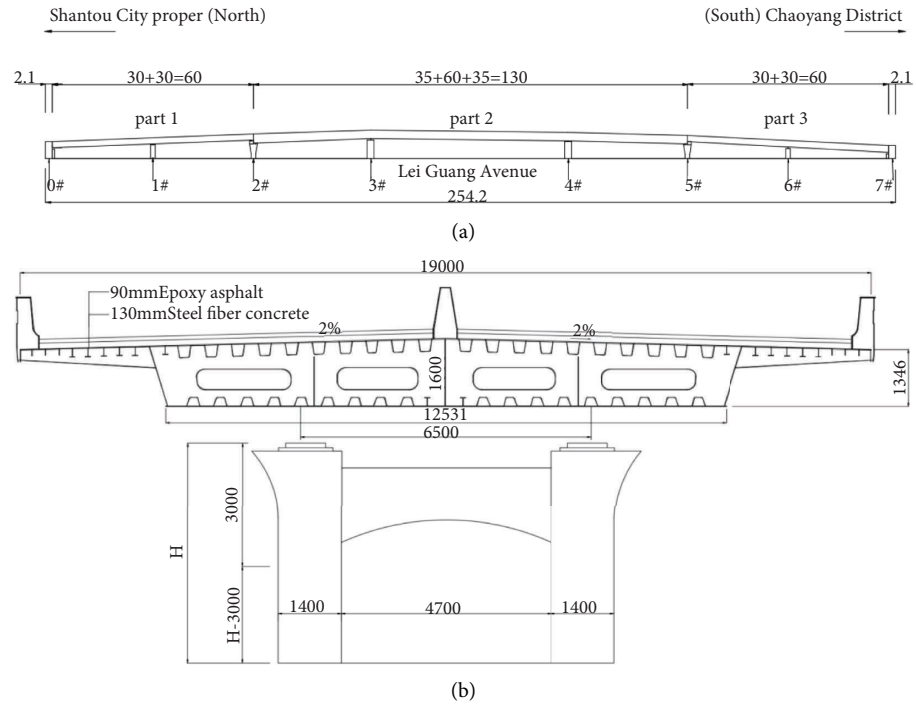

Figure 1: Layout of Leiguang Bridge and cross section of steel box girder. (a) Bridge elevation (unit: m). (b) Cross section of steel box girder and double-column pier (unit: mm).

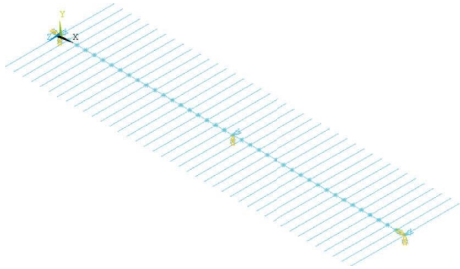

Figure 2: Initial finite element.

5. Modal Test and Analysis of Real Bridge

The modal parameters of the bridge were identified by the ambient excitation method [19]. The excitation signals of the ambient excitation method could be assumed as the white noise. Based on its characteristic of zero mean value, the frequency response function can be approximately replaced by the power spectral density function or the power spectral density function normalized by the multipoint average [20]. In this study, the measurement points were arranged in the box girders to avoid affecting the traffic on the bridge deck. Vertical and lateral vibration tests were carried out.

A total of 8 DH 991B vertical accelerometers were used in this study. The reference point sensor was numbered V0, and other sensors were numbered in the form of Va-b, with a indicating the test batch and b indicating the serial number of the sensor in the batch. The sampling frequency was 50 Hz, and the sampling duration for a single batch was 60 minutes. All sensors picked up vibration vertically. With the sensors placed upward, six measurement points were equally placed in the bridge span, symmetrical to the center line of the road across the bridge, and with distance of 5 m in the bridge longitudinal direction. In order to obtain the modal data reasonably, as limited by the number of sensors, the cross-point power spectrum method was used to record the data in batches, and each batch of data was analyzed in the DHDAS dynamic signal acquisition and analysis system, with the V0 measurement point as the reference point of all batches. A total of 20 points were actually measured on-site, and the test arrangement is as shown in Figure 4, where the triangles represent the first batch of measurement points (including reference point), the circles represent the second batch of measurement points, and the diamonds represent the third batch of measurement points.

Figure 5 shows the acceleration time history signals of the reference point V0 and V1-4 in the first batch obtained by the data acquisition system. The time domain data were FFT transformed to obtain the frequency domain data. The number of FFT analysis points was 1024, the window type was rectangular, and the overlap rate was 50%. Considering the results of finite element analysis, the peak points on the spectrum diagram were selected as the natural frequency of the structure, as shown in Figure 5, then the damping ratio at the natural frequency was obtained by the cross-power spectrum half-power bandwidth method, and then the mode at the natural frequency was obtained from the transmission rate and the phase diagram of the cross-power spectrum. Figure 6 gives the measured first six order modal mode shapes of the bridge and the corresponding frequencies.

Table 1: Bridge mode from FEM in comparison with measured results.

Modal order	FEM (Hz)	Mode shape	Measured frequency (Hz)	Difference (%)
1	3.77	First-order asymmetric vertical bending	4.00	−5.75
2	4.99	First-order symmetric vertical bending	5.03	−0.79
3	5.30	First-order symmetric torsion	5.27	+0.57
4	7.47	First-order asymmetric torsion	7.23	+3.32
5	11.96	Second-order symmetric torsion	10.99	+8.83
6	14.95	Second-order asymmetric torsion	14.01	+6.71

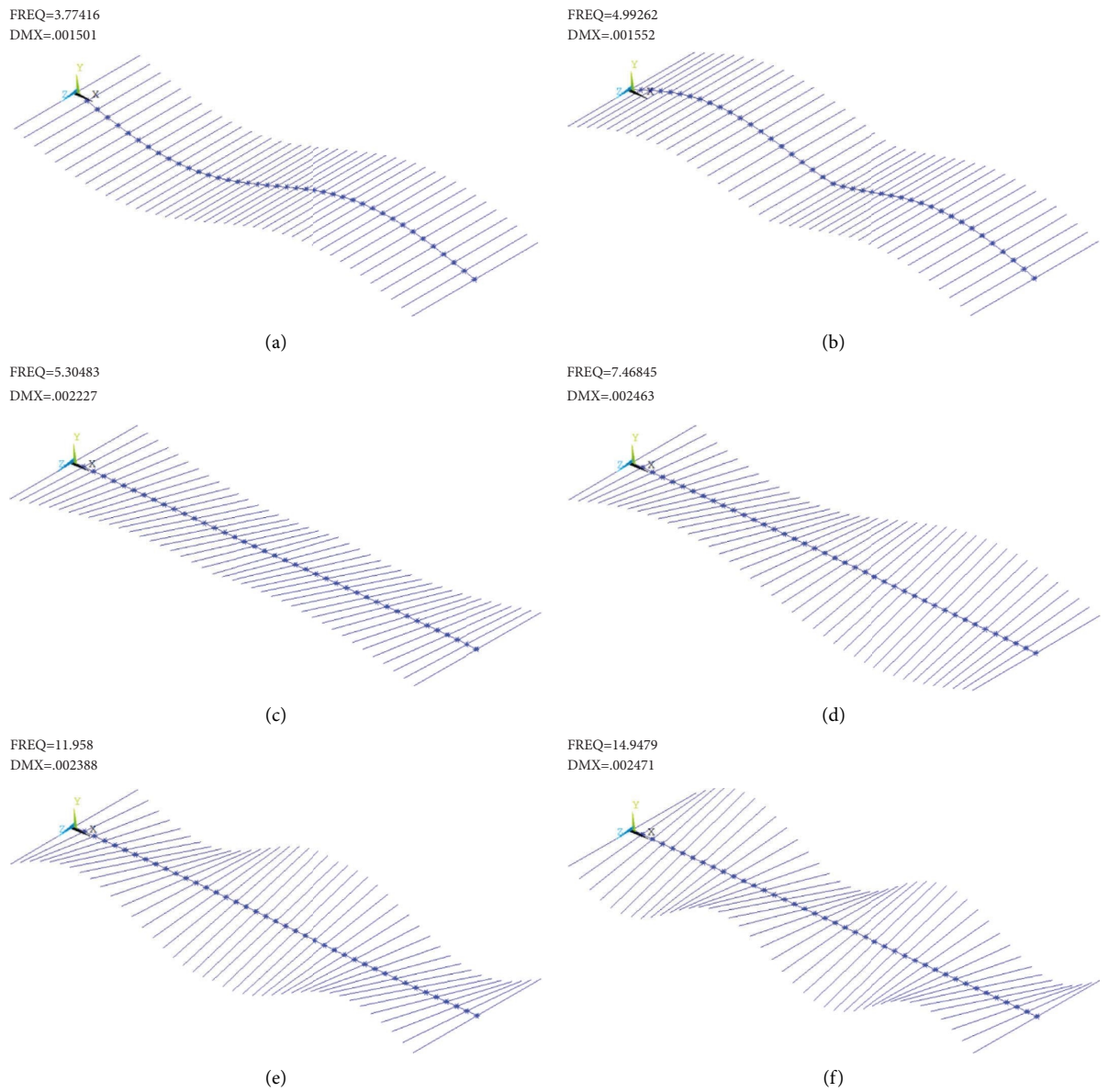

Figure 3: Calculated mode shape of the initial finite element model. (a) First-order asymmetric vertical bending (3.77 Hz). (b) First-order symmetric vertical bending (4.99 Hz). (c) First-order symmetric torsion (5.30 Hz). (d) First-order asymmetric torsion (7.47 Hz). (e) Second-order symmetric torsion (11.96 Hz). (f) Second-order asymmetric torsion (14.95 Hz).

As can be seen from Table 1, the measured mode shapes in this study were consistent with the results obtained by FEM analysis, and there was slight difference between the measured frequencies and the frequencies obtained from the initial finite element analysis, which shows that the finite element analysis based on the design drawings is reasonable. The measured basic mode of the bridge, that is, the first-order asymmetric mode, had a vertical bending frequency of 4.0 Hz, which was slightly higher than the FEM result of 3.77 Hz, with a difference of 5.75%. However, the basic

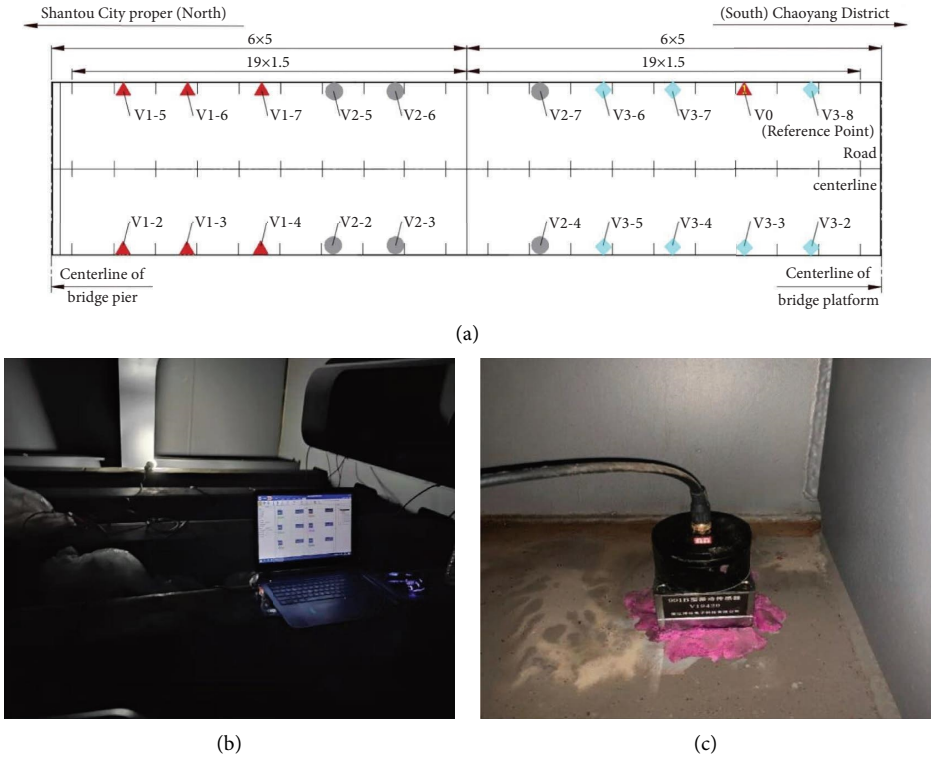

Figure 4: Test arrangement. (a) Vertical sensor arrangement (unit: m). (b) Data acquisition system in the steel box girder. (c) 991B acceleration sensor.

modes of the bridge according to the finite element analysis and field measurement were both significantly higher than the empirical value of $100/L$ (L is the bridge span in meters), which indicates that although the steel box girder of the bridge only had a height of 1.6 m, the vertical stiffness of the structure was relatively high, which may be improved by the SFRC layer pavement on the bridge deck. The finite element model simulated the 13 cm thick SFRC layer on the OSDs, while the vertical bending fundamental frequency in the finite element analysis was still lower than the measured value, which indicates that the SFRC layer on the bridge deck is no longer a traditional bridge deck pavement not considering stiffness but instead forms a steel-concrete composite structure together with the OSDs. Therefore, the structure formed by the SFRC layer with OSDs by means of shear studs must be simulated as a composite structure in the finite element model. The measured frequencies at the second-order antisymmetric torsion and the second-order antitorsion were both lower than those obtained from the initial finite element analysis, with the difference reaching 8.83% and 6.71%, respectively, which indicates that the torsional stiffness of the finite element model may be too large. The comparison of other results is shown in Table 1. The difference between the finite element analysis and the measured results shows that the finite element model based on the dimensions on the design drawings is inconsistent with the bridge in operation. In order to provide a reasonable finite element model for the subsequent antiseismic analysis of the bridge, the finite element model needs to be updated. Therefore, it is necessary to reasonably update the structural design dimensions and material properties of the real bridge on which the finite element model is based so that the finite element model can give results closer to the measured modes.

6. Finite Element Model Updating

6.1. Selection of Model Updating Parameters. According to the actual conditions of the Leiguang Overpass Bridge, the field investigation shows that the actual structural dimensions of the bridge are consistent with the design drawings, so the structural dimensions of the bridge were not selected as parameters to be updated. It could occur during the construction of the bridge that other structural parameters of the bridge did not match the recommended values of the design specifications. Therefore, the elastic modulus of steel of the steel box girder, the elastic modulus, thickness and density of SFRC, and the elastic modulus of the bridge deck epoxy asphalt (the temperature of the pavement changes with sunlight and the elastic modulus of the epoxy pavement decreases as the temperature rises) were proposed as the structural parameters to be updated. The initial values of the finite element model for these structural parameters to be updated are shown in Table 2. Taking the first six natural frequencies of the bridge as the characteristic values, the design method of the Box–Behnken design (BBD) numerical test was adopted. According to engineering experience, the proposed variation ranges of parameters to be updated are shown in Table 2.

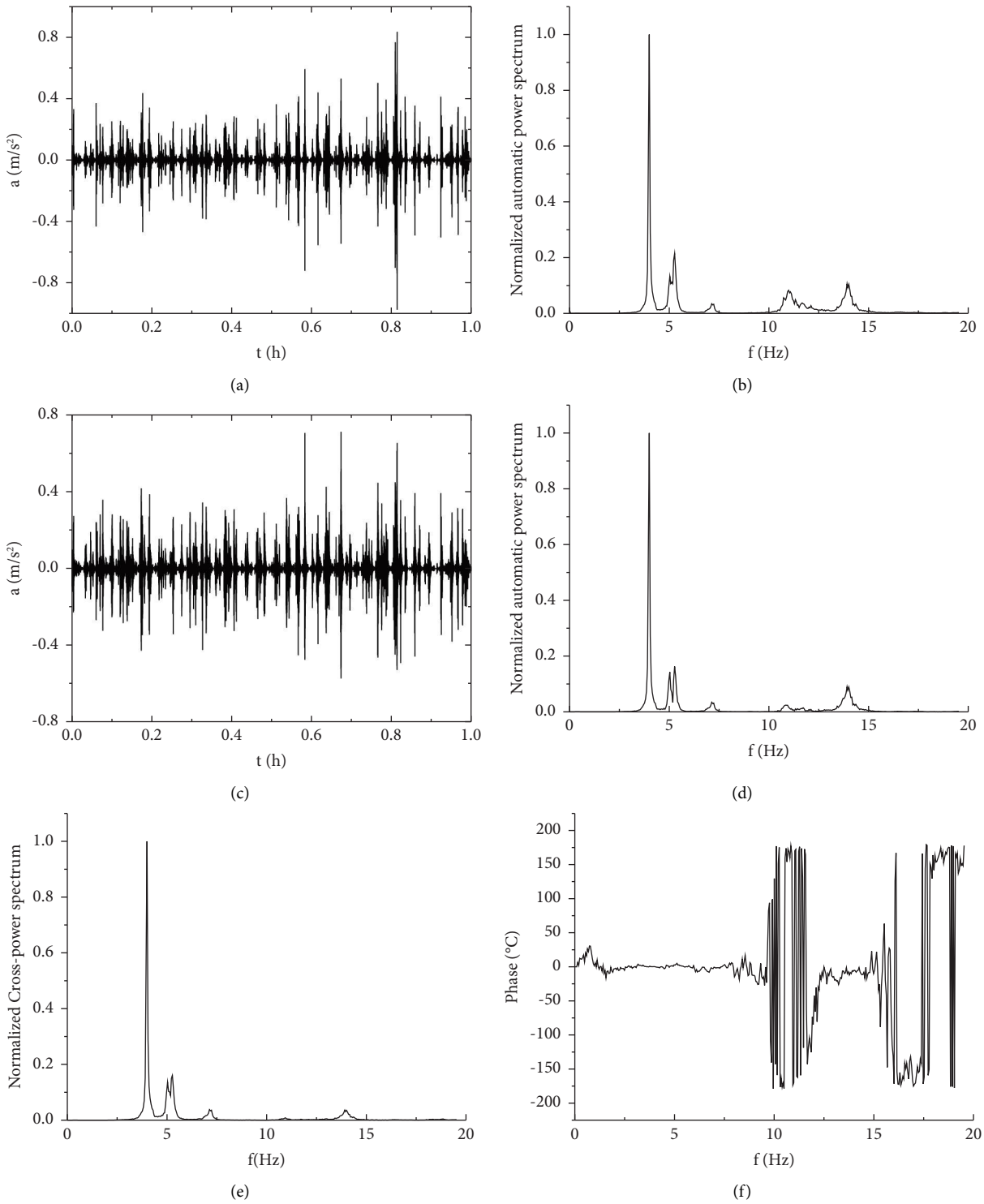

Figure 5: Measured time histories and their spectrum analysis. (a) Time course of acceleration at reference point V0. (b) Automatic power spectrum of the reference point V0. (c) Time course of acceleration across midpoint V1-4. (d) Automatic power spectrum for reference points V1-4. (e) Cross-power spectrum of the midspan measuring point V1-4 and the reference point V0. (f) Reference point V0 and cross-center V1-4 mutual power phase spectrum.

6.2. Significance Analysis. Each updating parameter is first screened out according to equation (1). If $P < 0.05$, it indicates that the updating parameter has a significant effect on the bridge frequencies; otherwise, it has no significant effect. The corresponding P values reflecting the effect of each updating parameter on the bridge frequencies are shown in Figure 7, where A, B, C, D, and E, respectively, represent the SFRC elastic modulus, SFRC

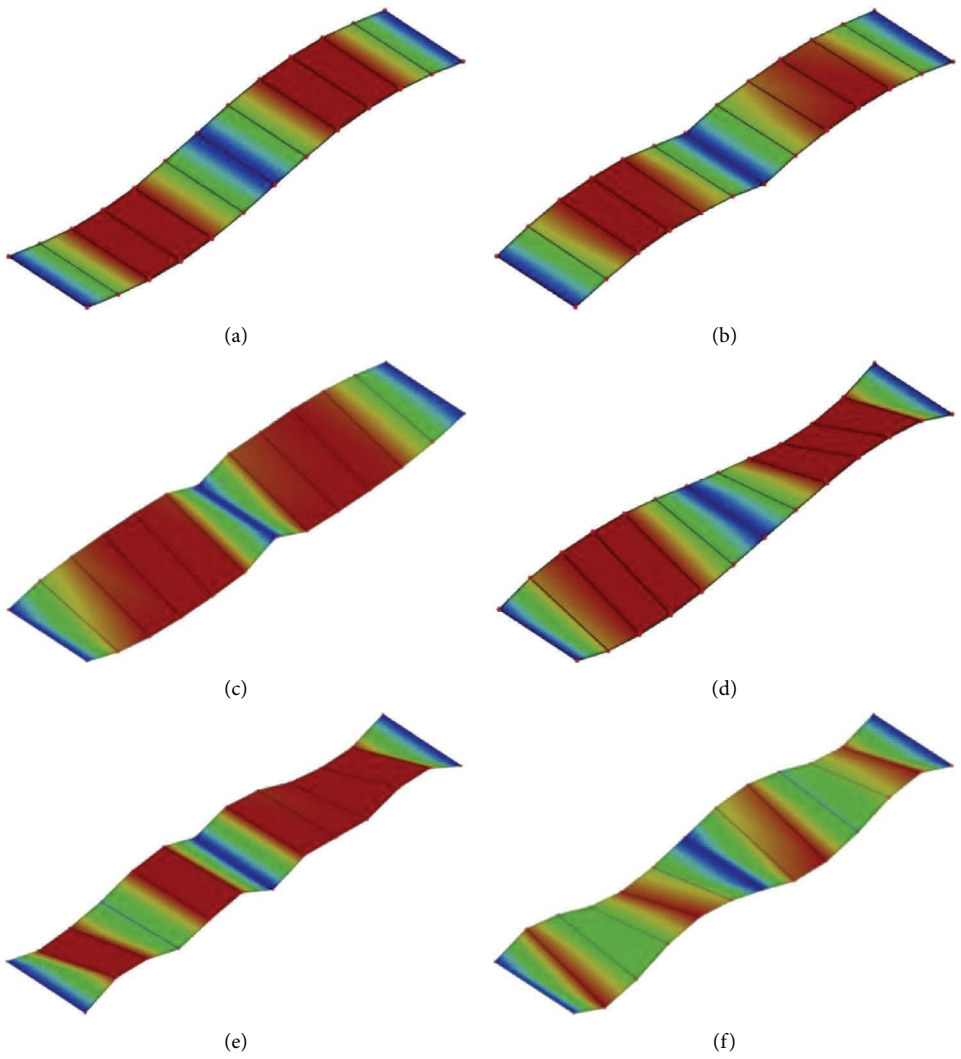

Figure 6: Measured bridge vibration modes. (a) First-order asymmetric vertical bending (3.77 Hz). (b) First-order symmetric vertical bending (4.99 Hz). (c) First-order symmetric torsion (5.30 Hz). (d) First-order asymmetric reversal (7.47 Hz). (e) Second-order symmetric torsion (11.96 Hz). (f) Second-order asymmetric reversal (14.95 Hz).

Table 2: Range of updated structural parameters.

Updating parameters	Modulus of elasticity of SFRC ($\times 10^4$ MPa)	Density of SFRC (kg/m^3)	Thickness of SFRC (mm)	Temperature of epoxy asphalt (°C)	Modulus of elasticity of steel box girder ($\times 10^5$ MPa)
Initial value	3.45	2400	130	30	2.1
Variation range	(2.9, 4)	(2000, 2800)	(100, 160)	(0, 60)	(1.68, 2.52)

density, SFRC thickness, epoxy asphalt temperature, and elastic modulus of steel of the steel box girder. From Figure 7, it can be seen that A, B, C, and D all have a significant effect on the first six natural frequencies, and E has a significant effect on the first three natural frequencies and the fifth natural frequencies, the interaction term BC has a significant effect on all the first six natural frequencies, BE and CE have a significant effect on the first two natural frequencies, the quadratic term DD has a significant effect on all the first six natural frequencies, and BB, CC, and EE have a significant effect on the first three natural frequencies. Obviously, on the premise of not affecting the accuracy of the response surface, it is necessary to select updating parameters that have a significant effect on the bridge mode.

6.3. Response Surface Fitting. The response surface fitting was carried out by using the numerical test design software design-expert (test data in supplementary materials) and the quadratic polynomial and the first four order regression response surfaces of the response surface model were obtained, as shown in Figure 8. The three coordinate axes of the space surface are the frequency values in the design space and the values of another two updating parameters,

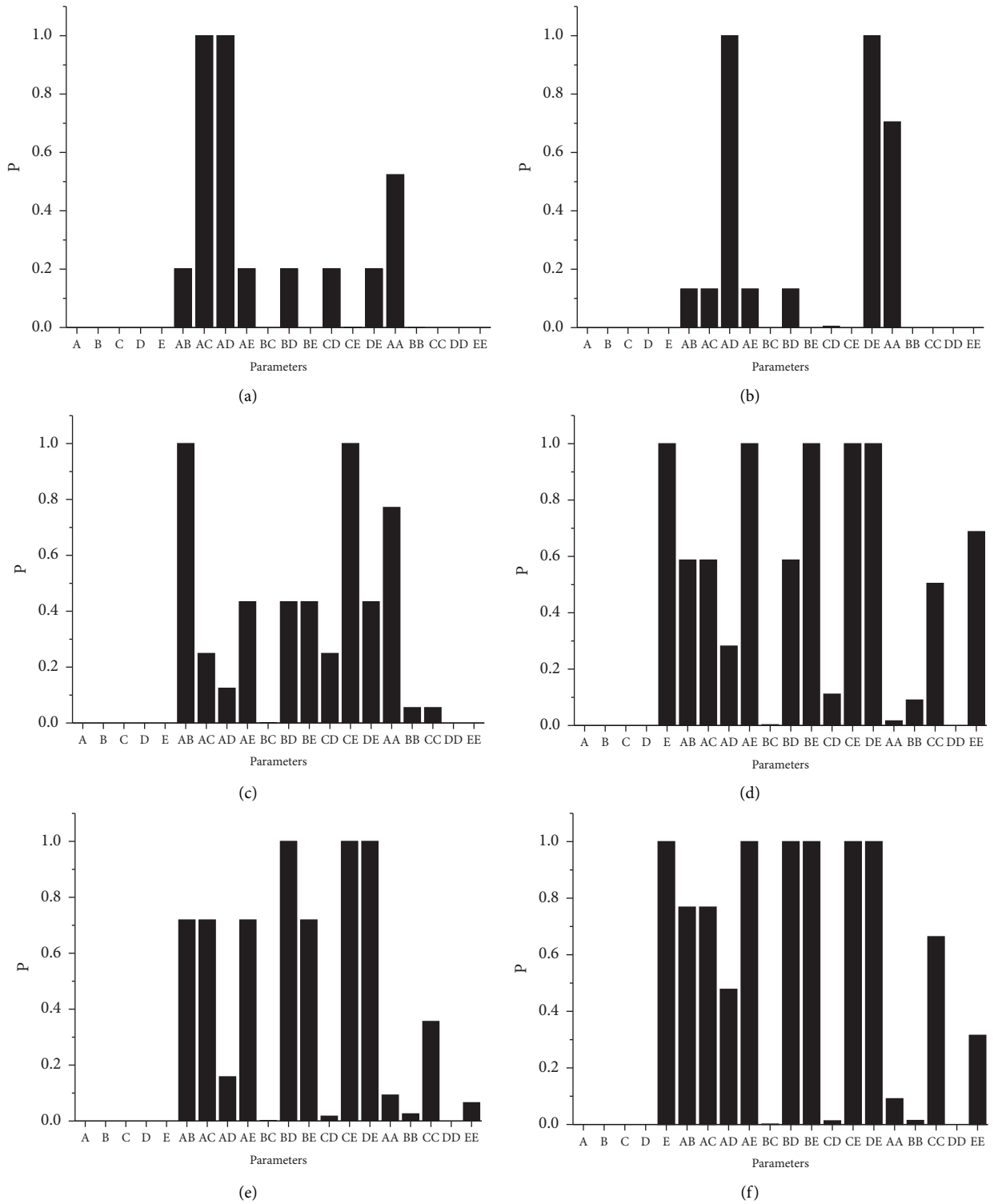

Figure 7: Significance of updating parameters for each order of frequency. (a) Significance of the updating parameter for the first-order frequency. (b) Significance of updating parameters for second-natural frequencies. (c) Significance of the updating parameter for the third-order frequency. (d) Significance of the updating parameter for the fourth-order frequency. (e) Significance of the updating parameter for the fifth-order frequency. (f) Significance of the updating parameter for the sixth-order frequency.

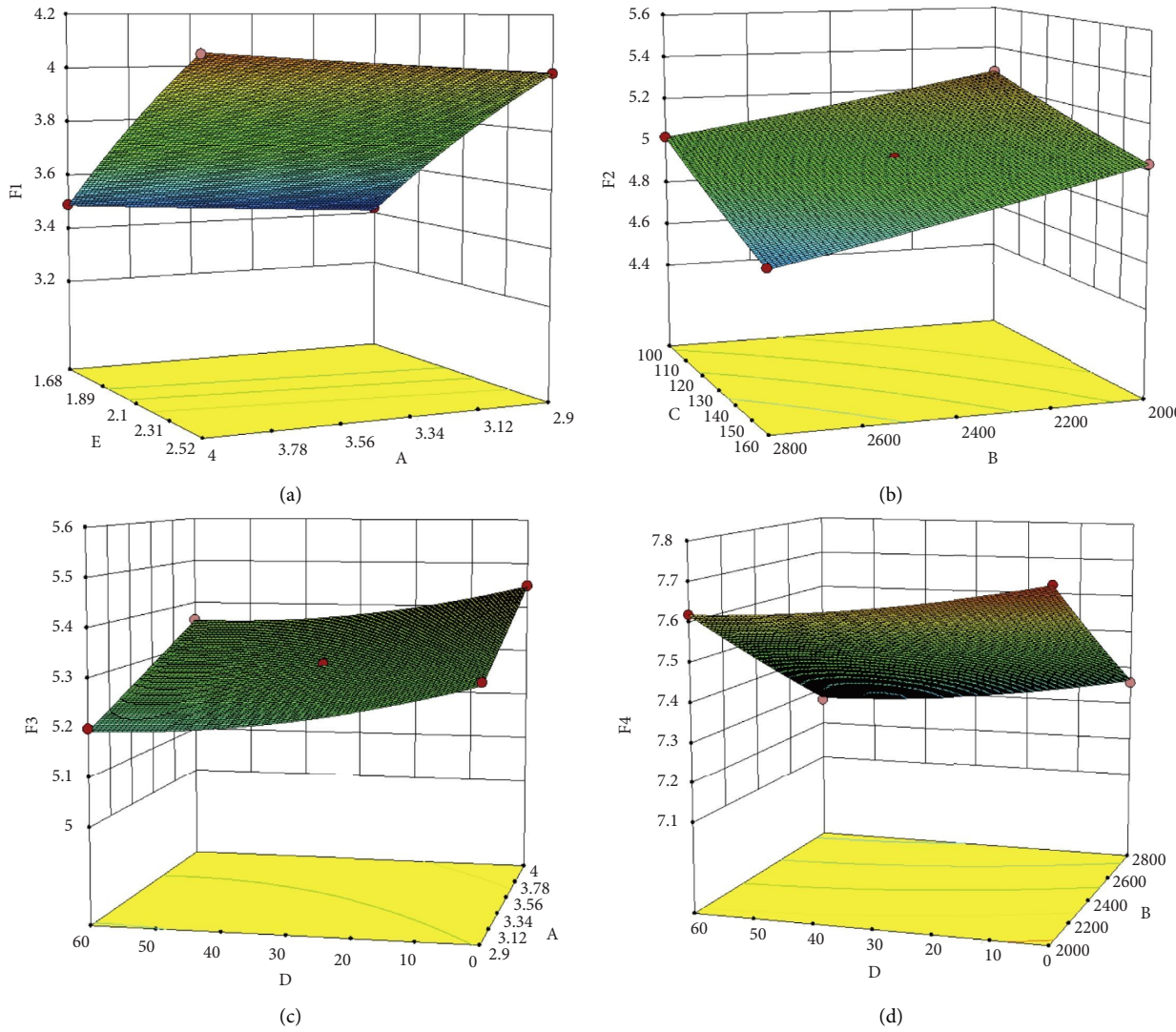

Figure 8: Regression response surface for each order of frequency. (a) f_1 and AE response surface. (b) f_2 and BC response surface. (c) f_3 and AD response surface. (d) f_4 and BD response surface.

respectively. The effect of the change of the parameters to be updated on the frequency of each order can be analyzed according to the trend of the surface and the characteristics of contour lines.

As can be seen from Figure 8, the SFRC elastic modulus has a positive effect on the first and third natural frequencies of the bridge, which may be related to the fact that the increase of SFRC elastic modulus in this bridge deck composite structure can increase the stiffness of the bridge. The SFRC density and thickness have negative effects on the second and fourth natural frequencies of the bridge because the increase of SFRC density and thickness increases the mass of the bridge, thus reducing the frequencies of the bridge. The temperature of epoxy asphalt has an overall negative effect on the third and fourth natural frequencies of the bridge, but when it is higher than 30°C, this effect is not obvious. This may be because the elastic modulus of epoxy asphalt is relatively high when the temperature is low and decreases significantly with the increase of temperature [3], thus not contributing additional stiffness to the OSDs. Among them, the SFRC thickness has the most significant effect on the bridge frequencies, and thus, the finite element model should accurately simulate the thickness of the SFRC pavement layer.

6.4. Accuracy Test and Parameter Optimization of the Response Surface. Whether the response surface model obtained by fitting is reasonable needs to be verified, and the accuracy test of the established response surface model was carried out by using the multiple correlation coefficient R^2 and the relative root mean square error (RMSE). The corresponding values obtained are shown in Table 3.

The results in Table 3 show that the R^2 value of each order frequency approaches 1 and the RMSE value approaches 0, indicating that the response surface model at each order frequency has high accuracy and can replace the initial finite element model in the calculation of the bridge mode under different updating parameters.

Table 3: Verification of the response surface model.

	f_1	f_2	f_3	f_4	f_5	f_6
R^2	1	0.9999	0.9978	0.9938	0.9987	0.9845
RMSE	0.0034	0.0057	0.0062	0.0047	0.0032	0.0065

Table 4: Final value of the updated parameter for the FEM model.

Updating parameters	Temperature of epoxy asphalt (°C)	Thickness of SFRC (mm)	Modulus of elasticity of SFRC ($\times 10^4$ MPa)	Density of SFRC (kg/m^3)	Modulus of elasticity of the steel box girder ($\times 10^5$ MPa)
Initial value	30	130	3.45	2400	2.1
Updated value	40.6	115.6	3.65	2781	2.25
Changes	+10.6	−14.4	+0.20	+381	+0.15

Table 5: Comparison of results before and after modal parameter updating.

Modal order	Measured frequency (Hz)	Mode shape	Modal damping ratio (%)	FEM before updating (Hz)	Difference (%)	GA-updated FEM (Hz)	Difference (%)
1	4.00	First-order asymmetric vertical bend	1.61	3.77	−5.75	3.88	−3.00
2	5.03	First-order symmetric vertical bend	4.76	4.99	−0.79	5.08	+0.99
3	5.27	First-order symmetric torsion	5.18	5.30	+0.57	5.26	−0.18
4	7.23	First-order asymmetric reversal	2.38	7.47	+3.32	7.38	+2.07
5	10.99	Second-order symmetric torsion	4.12	11.96	+8.83	11.83	+7.64
6	14.01	Second-order asymmetric reversal	2.04	14.95	+6.71	14.77	+5.42

The genetic algorithm (GA) is selected by using the MATLAB optimization toolbox for iterative updating within the response surface model, and the updated values of each design parameter after updating are shown in Table 4. The updated parameters are within the ranges of the parameters in Table 2 and are therefore valid updated values.

The updated structural parameters were reanalyzed by FEM, and the results were compared with the measured frequencies and the initial FEM results, as shown in Table 5. Except for the slight increase of the updated value at the second-order frequency, the other natural frequencies of the finite element model are all among the initial model results and the measured results; that is, the frequencies after updating are relatively close to the measured results, especially for the low-order modal frequencies of the bridge. This provides a more reasonable finite element model for the antiseismic analysis of bridges located in strong earthquake areas and also proves the rationality of the method in this paper.

7. Conclusions

Through the modal identification and model updating of the steel box-girder bridge with steel-SFRC composite decks, the study of the effect of the pavement in this kind of structures on the dynamic characteristics of the bridge and the response surface-based model updating with the SFRC elastic modulus, density, thickness, and epoxy asphalt temperature as the updating parameters help us to reach the following conclusions:

(1) Based on the measured bridge response under ambient excitation, the modal parameter identification method presents reasonable multiorder modal parameters of the actual bridge without artificial excitation, and these measured modal parameters provide the targets of updating for the bridge finite element model.

(2) Although the steel box-girders of the test bridge are of a small height, the fundamental frequency of the bridge is high and the vertical stiffness of the structure is large, indicating that the SFRC layer on the bridge deck is no longer a traditional bridge deck pavement that does not contribute stiffness but instead forms a steel-concrete composite structures with the OSDs. Therefore, the structure formed by the SFRC layer with the OSDs through shear studs must be reasonably simulated in the finite element model to reasonably reflect the contribution of the SFRC layer to the stiffness of the bridge.

(3) The updated parameters of the model (SFRC modulus of elasticity, density, thickness, and epoxy asphalt pavement temperature) all have an effect on the

first six orders of natural frequencies. Among them, SFRC thickness has the most significant effect on the bridge frequency. The effect of epoxy asphalt pavement on the bridge frequency is small, and even smaller above 30°C. Therefore, the finite element model should be able to accurately reflect the SFRC pavement thickness of the real bridge. The updated natural frequencies are relatively close to the measured results, especially for the basic natural frequencies of the bridge. This provides a more reasonable finite element model for the antiseismic analysis of bridges located in strong earthquake areas and also proves the rationality of the finite element analysis and the response surface-based model updating method.

Abbreviations

OSDs: orthotropic steel decks
SFRC: Steel fiber-reinforced concrete
FEM: Finite element model.

Data Availability

The data used to support the findings of the study are included within the article.

Conflicts of Interest

The authors declare that they have no conflicts of interest.

Supplementary Materials

The numerical test data of Box–Behnken Design are shown in Table 6. Table 6 Box–Behnken Design. (*Supplementary Materials*)

References

[1] Z. W. Zhu, Z. Xiang, J. P. Li, and A. Carpinteri, "Fatigue damage investigation on diaphragm cutout detail on orthotropic bridge deck based on field measurement and FEM," *Thin-Walled Structures*, vol. 157, Article ID 107106, 2020.

[2] Z. W. Zhu, J. P. Li, X. W. Chen, and A. Carpinteri, "Stress behaviors of rib-to-deck double-sided weld detail on orthotropic steel deck," *Journal of Constructional Steel Research*, vol. 187, Article ID 106947, 2021.

[3] S. Teixeira de Freitas, H. Kolstein, and F. Bijlaard, "Composite bonded systems for renovations of orthotropic steel bridge decks," *Composite Structures*, vol. 92, no. 4, pp. 853–862, 2010.

[4] Z. Xiang and Z. W. Zhu, "Simulation study on fatigue behavior of wrap-around weld at rib-to-floorbeam joint in a steel-UHPC composite orthotropic bridge deck," *Construction and Building Materials*, vol. 289, Article ID 123161, 2021.

[5] Z. W. Zhu, T. Yuan, Z. Xiang, Y. Huang, Y. E. Zhou, and X. Shao, "Behavior and fatigue performance of details in an orthotropic steel bridge with UHPC-deck plate composite system under in-service traffic flows," *Journal of Bridge Engineering*, vol. 23, no. 3, Article ID 04017142, 2018.

[6] X. M. Kong, Y. l. Liu, Y. R. Zhang, Z. l. Zhang, P. Y. Yan, and Y. Bai, "Influences of temperature on mechanical properties of cement asphalt mortars," *Materials and Structures*, vol. 47, no. 1-2, pp. 285–292, 2014.

[7] C. Yin, H. Zhang, and Y. Pan, "Cracking mechanism and repair techniques of epoxy asphalt on steel bridge deck pavement," *Transportation Research Record: Journal of the Transportation Research Board*, vol. 2550, no. 1, pp. 123–130, 2016.

[8] Y. Zhang and Z. C. Hou, "A model updating method based on response surface models of reserved singular values," *Mechanical Systems and Signal Processing*, vol. 111, pp. 119–134, 2018.

[9] W. X. Ren and H. B. Chen, "Finite element model updating in structural dynamics by using the response surface method," *Engineering Structures*, vol. 32, no. 8, pp. 2455–2465, 2010.

[10] B. A. Zárate and J. M. Caicedo, "Finite element model updating: multiple alternatives," *Engineering Structures*, vol. 30, no. 12, pp. 3724–3730, 2008.

[11] S. E. Fang and R. Perera, "Damage identification by response surface based model updating using D-optimal design," *Mechanical Systems and Signal Processing*, vol. 25, no. 2, pp. 717–733, 2011.

[12] L. Deng and C. S. Cai, "Bridge model updating using response surface method and genetic algorithm," *Journal of Bridge Engineering*, vol. 15, no. 5, pp. 553–564, 2010.

[13] Z. Xiang and Z. W. Zhu, "Multi-objective optimization of a composite orthotropic bridge with RSM and NSGA-II algorithm," *Journal of Constructional Steel Research*, vol. 188, Article ID 106938, 2022.

[14] Q. Fei, A. Li, X. Han, and C. Miao, "Modal identification of long-span Runyang Bridge using ambient responses recorded by SHMS," *Science in China - Series E: Technological Sciences*, vol. 52, no. 12, pp. 3632–3639, 2009.

[15] F. Wang, G. H. Huang, Y. Fan, and Y. P. Li, "Robust subsampling ANOVA methods for sensitivity analysis of water resource and environmental models," *Water Resources Management*, vol. 34, no. 10, pp. 3199–3217, 2020.

[16] T. K. Kim, "Understanding one-way ANOVA using conceptual figures," *Korean J Anesthesiol*, vol. 70, no. 1, pp. 22–26, 2017.

[17] G. Nastasi, V. Colla, S. Cateni, and S. Campigli, "Implementation and comparison of algorithms for multi-objective optimization based on genetic algorithms applied to the management of an automated warehouse," *Journal of Intelligent Manufacturing*, vol. 29, no. 7, pp. 1545–1557, 2018.

[18] Q. Yuan and F. Qian, "A hybrid genetic algorithm for twice continuously differentiable NLP problems," *Computers & Chemical Engineering*, vol. 34, no. 1, pp. 36–41, 2010.

[19] J. Chang and S. Nagarajaiah, "Quantum-behaved particle swarm optimization-based structural modal parameter identification under ambient excitation," *International Journal of Structural Stability and Dynamics*, vol. 16, no. 05, Article ID 1550008, 2016.

[20] Y. F. Liu, K. Xin, J. S. Fan, and D. Y. Cui, "A review of methods for identifying structural modal parameters under environmental excitation," *Engineering Mechanics*, vol. 31, pp. 46–53, 2014.

[21] G. Kaliyaperumal, B. Imam, and T. Righiniotis, "Advanced dynamic finite element analysis of a skew steel railway bridge," *Engineering Structures*, vol. 33, no. 1, pp. 181–190, 2011.